ACS APPLIED MATERIALS & INTERFACES

www.acsami.org

Research Article

Fouling Resistance and Release Properties of Poly(sulfobetaine) Brushes with Varying Alkyl Chain Spacer Lengths and Molecular Weights

Fahimeh Khakzad, Narendra K. Dewangan, Tzu-Han Li, Farshad Safi Samghabadi, Ronard Herrera Monegro, Megan L. Robertson,* and Jacinta C. Conrad*

Cite This: *ACS Appl. Mater. Interfaces* 2023, 15, 2009−2019

Read Online

ACCESS | Metrics & More | Article Recommendations | Supporting Information

ABSTRACT: We examined the effects of alkyl carbon spacer length (CSL) and molecular weight on fouling resistance and release properties of zwitterionic poly(sulfobetaine methacrylate) brushes. Using surface-initiated atom transfer radical polymerization, we synthesized two series of brushes with CSL = 3 and 4 and molecular weight from 19 to 1500 kg ·mol^{-1}, corresponding to dry brush thickness from around 6 to 180 nm. The brush with CSL = 3 was nearly completely wet with water (independent of molecular weight), whereas the brush with CSL = 4 exhibited a strong increase in water contact angle with molecular weight. Though the two-brush series had distinct wetting properties, both series of brushes exhibited similarly great resistance against fouling by *Staphylococcus epidermidis* bacteria and *Aspergillus niger* fungi spores when submerged in water, indicating that neither molecular weight nor CSL strongly affected the antifouling behavior. We also compared the efficacy of brushes against fouling by fungi and silicon oil in air. Brushes grafted to filter paper were strongly fouled by fungi and silicon oil in air. Grafting the polymers to the filter paper, however, greatly enhanced removal of the foulant upon rinsing. The removal of fungi and silicon oil when rinsed with a salt solution was enhanced by 219 and 175%, respectively, as compared to a blank filter paper control. Thus, our results indicate that these zwitterionic brushes can promote foulant removal for dry applications in addition to their well-known fouling resistance in submerged conditions.

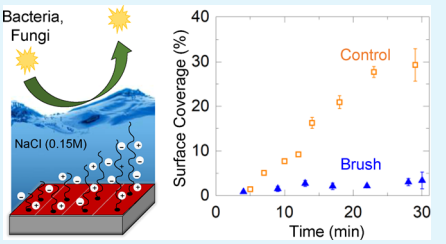

KEYWORDS: *zwitterionic polymer brush, 3-(N-2-methacryloyloxyethyl-N,N-dimethyl) ammonatopropanesulfonate (MAPS), 3-(N-2-methacryloyloxyethyl-N,N-dimethyl) ammonatobutanesulfonate (MABS), polyMAPS, polyMABS, Aspergillus niger, Staphylococcus epidermidis*

1. INTRODUCTION

Inspired by their structural similarities to phospholipid bilayers of blood cells,[1] polyzwitterions are widely used in fouling-resistant coatings. Polyzwitterions (such as poly(phosphobetaine)s, poly(carboxybetaine)s, and poly(sulfobetaine)s) are charge-neutral with high charge density, containing positively and negatively charged groups linked together with an alkyl chain spacer.[2−5] These charged groups can undergo both hydrogen bonding and electrostatic bonding with water molecules, which makes polyzwitterions good candidates for applications in lubricants or fouling-resistant coatings. When used as a coating, polyzwitterions provide a strong and dense water layer over the treated surface, acting as an energy barrier, preventing strong contact with foulants and inhibiting most adhesion phenomena.[6−10]

The solubility and surface wettability of polyzwitterions are affected by chain associations that are driven by inter- and intra-chain Coulomb interactions.[11,12] These electrostatic interactions increase in strength with both molecular weight and polymer concentration, thereby increasing the upper critical solution temperature (UCST) of the polymer.[13] The presence of salts can lead to an anti-polyelectrolyte effect with charge screening and facilitate hydration of the polymer.[14−16] The alkyl carbon spacer length (CSL) is an important factor in hydration and solubility of these polymers: an increase in CSL strengthens hydrophobicity and also electric potential, reducing hydration.[17] Although these parameters have been studied in the context of polymer solubility and hydration, their impact on fouling properties of polyzwitterionic coatings is not well understood.

Polyzwitterionic brushes have even more favorable attributes as coatings, as covalently bonding the chains to a surface provides durability and enables mechanisms such as steric hindrance that promote fouling-resistant behavior.[18,19] The hydration and surface wettability of polyzwitterionic brushes

Received: September 12, 2022
Accepted: December 6, 2022
Published: December 19, 2022

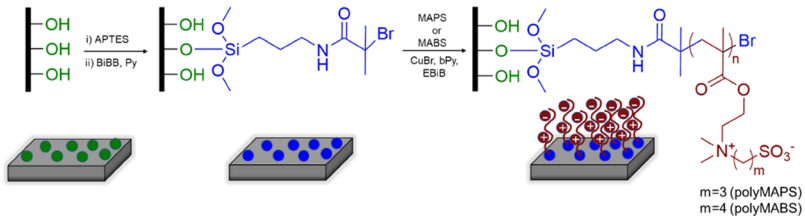

Figure 1. Synthesis of polyMAPS or polyMABS through initiator immobilization followed by SI-ATRP.

are key factors governing their fouling resistance.[20] An increase in CSL decreases surface wettability with water, which is attributed to reduced solubility and slower dynamics of hydration.[7] By contrast, the impact of molecular weight and brush thickness on surface wettability and hydration is not as clearly understood. For example, one study identified a pronounced transition from hydrophilic to hydrophobic at a critical brush thickness in poly(sulfobetaine) brushes with CSL = 3,[21] whereas another study reported a constant hexadecane contact angle of around ∼10° over a broad range of brush thicknesses.[22] Thus, it is still not clear how variations in brush thickness or molecular weight affect surface wettability and hydration of polyzwitterionic brushes and if these properties are correlated to their fouling behavior.

The fouling resistance of polyzwitterionic brushes has been explored in the context of brush properties. An optimal film thickness for poly(sulfobetaine) brushes (CSL = 3) was found to minimize protein adsorption.[23] Fouling on polycarboxybetaine brush surfaces of similar thickness, but with longer CSL, was shown to be more affected by changes in ionic strength and foulant type.[24,25] Similar sensitivity to both CSL and salt concentration on protein adsorption was shown in poly(sulfobetaine) methacrylamide brushes with a similar thickness.[16] However, the effects of CSL and molecular weight, along with brush thickness, on fouling resistance are not fully elucidated. Additionally, most studies on fouling resistance of polyzwitterionic coatings have been conducted in submerged conditions, in which the brushes are fully hydrated, and the resistance of these surfaces to contamination in air, relevant to real-world coating applications, has been rarely investigated.[26−28]

Incorporation of poly(sulfobetaine)s has shown to facilitate fouling release from affected surfaces. Thin poly(sulfobetaine) surface layers promoted the detachment of surface-bound bacteria,[29] and grafted poly(sulfobetaine) enabled the release of attached marine microorganisms[30,31] and silicon oil[32] from submerged surfaces. Poly(sulfobetaine)s added to coating formulations have also been shown to enhance fouling removal.[33] The effect of CSL and type of foulant, however, on the efficacy of fouling release is less studied.

In this study, we focus on the fouling resistance and release properties of poly(sulfobetaine) brushes, which are appealing candidates for coatings due to their chemical stability, nearly pH-independent zwitterionic character, and biocompatibility,[14,34] and examine the impact of brush parameters on fouling resistance and release. First, we investigated the effects of molecular weight (19−1500 kg·mol^{-1}) and CSL (3, 4) on fouling of poly(sulfobetaine) brushes in the wet state by bacteria (*Staphylococcus epidermidis*) and fungi (*Aspergillus niger*). Although changing CSL altered the surface wettability, all brushes across a range of molecular weights exhibited high resistance to fouling by bacteria and fungi spores. Thus, neither molecular weight nor CSL strongly affected the (good) antifouling properties in submerged conditions. Furthermore, we investigated fouling and fouling release properties in air of the brushes attached to filter paper, using silicon oil and fungi as model foulants. Neither polyzwitterionic brush prevented fouling in air, but both brushes greatly enhanced the removal of fungi and oil after rinsing. Understanding of the fouling and fouling release properties of polyzwitterionic brushes of varying CSLs and molecular weights, in both dry (in air) and submerged states, is relevant to applications in medical devices, membrane technologies, and coatings.

2. MATERIALS AND METHODS

2.1. Materials. All reagents were obtained from Sigma Aldrich unless otherwise noted. 3-(N-2-methacryloyloxyethyl-*N*,*N*-dimethyl) ammonatopropanesulfonate (MAPS) and 3-(N-2-methacryloyloxyethyl-*N*,*N*-dimethyl) ammonatobutanesulfonate (MABS) monomers were synthesized following published protocols.[11] Triethylamine (TEA, ≥99.5%), 2-dimethylaminopyridine (DMAP, 97%), α-bromoisobutyryl bromide (BiBB, 98%), copper(I) bromide (CuBr, 98%), bipyridyl (bPy, ≥99%), pyridine (anhydrous, 99.8%), (3-aminopropyl)triethoxysilane (APTES, 99%), trifluoroethanol (TFE, ≥99%), 1-butyl-3-methylimidazolium chloride (BMImCl, ≥99%), and ethyl α-bromoisobutyrate (EbiB, 98%) were used as received unless otherwise noted. CuBr was purified according to a published procedure.[35] EBiB was degassed with three freeze−pump−thaw cycles. Thin plate silicon wafers (SSP, University Wafers ID 1080) were cut into approximately 1 × 2 cm pieces before use and together with glass coverslips (VWR, 22 × 40 × 0.15 mm) and filter paper (Whatman Grade 40) were used as polymer brush substrates. Dichloromethane (JT Baker, HPLC grade, 99.8%) was dried using a Pure Process Technology solvent purification system. Milli-Q water (Millipore Inc., Billerica, MA) with resistance of 18 MΩ cm^{-1} was used.

2.2. Brush Synthesis. *2.2.1. Initiator Immobilization Process on Glass Slides or Silicon Wafers.* Similar to our previous publication,[36] silicon wafers and glass coverslips were cleaned with acetone and water using a sonication bath. They were carefully dried with nitrogen flow and then exposed to air plasma for 5 min to activate the surfaces. Substrates were exposed to APTES at 50 mTorr for 30 min and then annealed at 110 °C for 30 min. Finally, to graft the initiator on the surface, the silanized substrates were immersed in 20 mL of dry dichloromethane containing 0.4 mL of anhydrous pyridine. 0.2 mL of BiBB was added dropwise at 0 °C to the solution in an ice bath and held for 1 h followed by 12 h at room temperature. The substrates were rinsed with acetone, dried under nitrogen, and transferred to the glovebox, under inert gas protection, to be used for polymerization.

2.2.2. Surface-Initiated Atom-Transfer Radical Polymerization of MAPS and MABS on Glass Slides or Silicon Wafers. In a typical protocol for the surface-initiated atom-transfer radical polymerization (SI-ATRP) of MAPS or MABS, a freshly prepared initiator-immobilized silicon wafer and glass coverslip were transferred to the glovebox in a 100 mL round bottom reaction flask. The silicon substrate was added to each reaction mixture to allow the dry brush thickness to be measured with ellipsometry; we assumed that the dry brush thicknesses on the glass coverslip and the silicon substrate were equal. CuBr, bPy, and EBiB (1:2:1 molar ratio) were added to the flask, which was then sealed with a septum and subsequently

https://doi.org/10.1021/acsami.2c16417
ACS Appl. Mater. Interfaces 2023, 15, 2009−2019

transferred out of the glovebox. Solutions of MAPS or MABS monomers were prepared separately by dissolving specified amounts of the monomer (Table S1) in 20 mL of TFE and 2.8 g of BMImCl (10 wt % relative to TFE) in a second sealed flask that was purged with nitrogen for 30 min. The de-aerated monomer mixture was then added to the flask containing the surfaces under nitrogen purge using a syringe. Next, the flask containing the surfaces was placed in an oil bath at 60 °C and its contents were stirred for 24 h to generate either polyMAPS or polyMABS brushes from the substrate and free (unbound) polymer (from free EBiB initiator) (Figure 1). The reaction was stopped by opening the flask to air at room temperature. The free polymer in solution was precipitated into methanol. The polymer-grafted substrates were washed with copious amounts of 0.5 M NaCl solution to remove any free polymer adsorbed on the surface, rinsed with deionized (DI) water and methanol, and dried with nitrogen.

2.2.3. Initiator Immobilization onto Filter Paper. We adopted published protocols[37,38] for esterification of hydroxyl groups of cellulose-based filter paper to immobilize the initiator. Four pieces of 1 × 2 cm paper were immersed in 50 mL of THF solution. TEA (4.44 g, 44 mmol) and DMAP (440 mg) were added to the flask. This reaction mixture was stirred in an ice bath. BIBB (9.2 g, 40 m mol) was then added into the mixture dropwise. The reaction proceeded at 0 °C for 1 h and then at room temperature for 24 h, with stirring. After the reaction, the initiator-functionalized filter papers were removed from the solution, thoroughly washed with dichloromethane and ethanol ultrasonically for 5 min each, and dried in a vacuum oven overnight.

2.2.4. SI-ATRP of MAPS and MABS on Filter Paper. In a similar approach to conducting SI-ATRP on glass slides or silicon wafers, four pieces of dry initiator-functionalized filter paper, CuBr (29 mg, 0.2 mmol), and bPy (62 mg, 0.4 mmol) were introduced into a dry flask inside a glovebox. A degassed solution of TFE, containing either MAPS or MABS (35 mmol), was then added into the flask using a syringe under nitrogen. SI-ATRP proceeded at 60 °C for 24 h. After the reaction, the polymer-grafted filter papers were removed from the solution, thoroughly washed with NaCl solution, distilled water, and methanol, and dried under vacuum. These brush syntheses were conducted in the absence of free EBiB initiator. The ratio of monomer to the ATRP catalyst was 35 mmol:0.2 mmol = 175:1.

2.3. Polymer and Brush Characterization. *2.3.1. Proton Nuclear Magnetic Resonance Spectroscopy.* Monomer conversion was measured after the polymerization reaction using proton nuclear magnetic resonance spectroscopy (^{1}H NMR). NMR spectra were collected on a JEOL ECA-500 spectrometer using 0.1 M NaCl solution in deuterated water (D_2O) as the solvent. Chemical shifts were referenced to the residual protonated water resonance (δ = 4.8 ppm).

2.3.2. Gel Permeation Chromatography. The weight- and number-average molecular weights (M_w and M_n, respectively) and dispersity ($Đ$=M_w/M_n) of the zwitterionic polymers formed in solution were determined by gel permeation chromatography (GPC). To remove unreacted monomer and other impurities, about 0.5 g of polymer was dissolved in 3 L of a 0.1 M NaCl solution and dialyzed (Spectrum Laboratories, Inc., Spectra/Por, MWCO 6−8 kDa) in 2 L of a 0.1 M NaCl solution. The dialysis bag was removed and then dialyzed in 2 L of DI water. GPC chromatograms were acquired with an aqueous triple detection Viscotek GPC system (VE 1122) equipped with two PL Aquagel-OH MIXED-M 8 mm columns (300 × 7.5 mm, Agilent) in series and including a refractive index detector (Viscotek VE-3580) and dual light scattering detector and viscometer (Viscotek 270) for absolute molecular weight determination [poly(ethylene oxide) and dextran standards acquired from Malvern Panalytical were used as narrow and broad standards, respectively, to calibrate the triple detection system]. The eluent consisted of 0.2 M $NaNO_3$ and 0.065 g·L^{-1} NaN_3 at room temperature. The eluent and the polymer solutions were filtered by nylon membrane filters (pore size 0.2 μm, Fisher Scientific) before being injected into the system. The flow rate was 1.0 mL·min^{-1}, and the injection volume was 20 μL.

2.3.3. Ellipsometry. The dry brush thickness was measured at three different locations on each silicon wafer substrate with a J.A. Woollam M-2000 spectroscopic ellipsometer. A three-layer model composed of silicon, silicon oxide (1.4 nm), and a transparent Cauchy layer ($n(\lambda) = A + B\,\lambda^{-2}$ (A and $B > 0$) was used. The polymer brush layer was modeled as a transparent dielectric layer with an absorption coefficient close to zero.

2.3.4. Contact Angle Measurement. Quasi-static advancing and receding contact angles and a metastable static contact angle were recorded with a Dataphysics OCA 15EC goniometer equipped with an inclinable stage to hold the sample and a camera for drop shape analysis. Quasi-static advancing and receding contact angles were measured using the expansion/shrinkage method according to the protocol in Ref 39. Briefly, a 2 μL droplet of MilliQ water was placed on the surface (silicon wafer or glass) using an automatic injector syringe, and the syringe tip was centered in the drop. 1 μL of MilliQ water was added to the droplet at a flow rate of 0.1 μL s^{-1} to reach a volume of 3 μL. After waiting for 10 s to ensure that the droplet was in equilibrium, MilliQ water was added to the droplet at a flow rate of 0.1 μL s^{-1} and the value of the advancing contact angle was determined from the advancing contact line. For the receding contact angle, water was withdrawn from the droplet at a flow rate of 0.1 μL s^{-1} and the value of the receding contact angle was determined from the receding contact line. For the static contact angle measurement, a 3.0 μL droplet of MilliQ water or NaCl solution was placed on the surface (filter paper, silicon wafer, or glass) using an automatic injector syringe. Measurements were conducted in ambient air at room temperature. The relative humidity was approximately 50%.

2.3.5. Attenuated Total Reflection-Fourier Transform Infrared Spectroscopy. Attenuated total reflection-Fourier transform infrared spectroscopy (ATR-FTIR) (Nicolet 6700) analysis was used to confirm polymer grafting onto filter paper. IR absorbance was recorded with OMNIC data acquisition software using 128 scans at a resolution of 8 cm^{-1}. To remove physically adsorbed polymers from the filter paper surface, the polymer-grafted filter paper was soaked in 0.1 M NaCl solution overnight, then soaked in DI water overnight, and subsequently dried prior to performing ATR-FTIR analysis.

2.4. Bacteria Deposition (Fouling) on polyMAPS and polyMABS Brushes on Glass Substrates. *2.4.1. Bacteria Culture Preparation.* *Staphylococcus epidermidis* (ATCC 12228) was used as a model bacterium. Luria−Bertani (LB) agar plates were made from 5 g of NaCl, 5 g of yeast extract, and 10 g of Bacto-tryptone mixed with 15 g of agar per 1 L water (all from BD Chemicals). Bacteria from a frozen stock were grown on these plates for 18 h at 37 °C. One colony was harvested and inoculated in the same LB medium and incubated in an orbital incubator shaker (SH1000, Southwest Science) at 37 °C and 200 rpm for about 10 h. Afterward, a secondary culture was prepared by diluting this culture 100-fold in LB medium and incubated for 12 h. Then, the culture was centrifuged at 5000 g to remove the supernatant growth media. The bacteria cell pellet was resuspended in 0.15 M NaCl (0.9 wt %, ionic strength 154 mM) and centrifuged again followed by removing the supernatant. The pellet was re-suspended in 0.15 M NaCl solution, and the optical density (OD) of the suspension was measured. Subsequently, 3 mL of a bacteria suspension with OD of 13.5 (Laxco DSM-Micro Cell Density Meter) was prepared. For imaging, the bacteria suspension was stained using SYTO 9 nucleic acid stain (Thermo Fisher) and later diluted with 0.15 M NaCl solution to reach a final OD of 0.9.

2.4.2. Bacteria Deposition. A flow cell for bacterial deposition experiments was assembled by attaching a control or polymer-grafted glass coverslip to a custom-machined polycarbonate flow cell of dimensions 1.2 mm × 30 mm × 3.8 mm with a silicone sealant (3 M), which was cured overnight.[40] The channels in the flow cell were filled with 0.15 M NaCl solution, and the substrates were allowed to equilibrate for 30 min. After equilibration, bacteria suspensions were flowed through the channel for 30 min using a syringe pump [Fusion 200 pump (Chemyx), 1 mL·min^{-1}]. Using a confocal fluorescence scanner (VT Infinity, Visitech) connected to a Leica DM4000 inverted microscope and a 40× oil immersion lens (HCX PL APO, NA 1.25−0.75), bacteria deposited on the substrates during flow were

https://doi.org/10.1021/acsami.2c16417
ACS Appl. Mater. Interfaces 2023, 15, 2009−2019

imaged over time. A laser excitation source of wavelength λ = 488 nm was used to excite the SYTO 9 nucleic acid stain. Using Voxcell Scan software (Visitech), 10 images were acquired [ORCA 200 camera (Hamamatsu)] at different locations in the $x-y$ plane of the flow cell for each experiment. The exposure time was 0.3 s, and the pixel size was 0.125 ± 0.001 μm.

2.5. Fungi Fouling and Fouling-Release on polyMAPS and polyMABS Brushes on Glass Substrates. *2.5.1. Aspergillus Niger Culture Preparation.* Resistance to fungi spore attachment was tested using *Aspergillus niger* (ATCC 6275). Following a published protocol,[41] the fungus was cultivated on oatmeal agar medium (Difco Oatmeal Agar, BD) and incubated at 28 °C for 4 days.

2.5.2. Aspergillus Niger Deposition Experiment on Glass Substrates. A chamber made of a glass slide (75 mm × 25 mm), a polydimethylsiloxane spacer (about 500 μm thick), and a plain or polymer-grafted glass coverslip was constructed for this study. To minimize adhesion of spores to the substrate, the base glass slide was made hydrophilic by treatment with air plasma (Harrick plasma cleaner PDC-32G) for 5 min prior to the attachment of the sample glass coverslip to the chamber. Subsequently, the sample glass coverslip was attached to this assembly using vacuum grease.

To prepare the fungi dispersion, spores were scraped from the nutrient agar using a sterile micropipette tip and mixed with 3 mL of 0.9 wt % saline by a vortex mixer until the spores were homogeneously dispersed. The OD of this suspension was adjusted to 0.5. Then, 20 μL of an *A. niger* spore suspension was injected into the chamber. Spores were allowed to attach to the sample glass coverslip for 25 min, after which the surface was imaged using brightfield microscopy. After this deposition step, the chamber was inverted and quickly imaged to quantify the number of spores that remained attached to the surface.

2.6. Fungi Fouling and Removal from polyMAPS and polyMABS Brushes on Dry Filter Paper. *2.6.1. Fouling Resistance.* Unmodified filter paper and polyMAPS-/polyMABS-grafted filter paper (approximately 1 × 2 cm) were disinfected using UV sterilization for 30 min. Then, three samples were placed onto each oatmeal agar medium plate (diameter of 9 cm) with sterile tweezers. 2 μL of an *A. niger* spore suspension was dropped on the center of the plate and cultured at 28 °C in an incubator. Fungal growth was observed and recorded with a digital camera (iPhone VI). For this test, each set of experiments was repeated at least three times.

2.6.2. Fungi Release. Using a home-made rinsing setup equipped with a spray nozzle (Figure S9), fungi-fouled filter paper samples were rinsed with 0.5 M NaCl solution at a constant flow rate of 60 mL·min^{-1} for 2 min. Images of the samples were acquired using the digital camera over the duration of rinsing. Using ImageJ software (National Institutes of Health), the images were converted to binary and the surface coverage (SC) by fungi for each image was calculated from the ratio of the area covered by fungi particles (black pixels) to the total image area (calculated from the number of pixels). The fungi removal (FR) percentage (removal from the surface) was calculated as

$$\mathrm{FR} = (1 - \mathrm{SC_R}/\mathrm{SC_F}) \times 100\% \quad (1)$$

where $\mathrm{SC_F}$ and $\mathrm{SC_R}$ are SC from the initial fouling and SC after rinsing the surface for 2 min, respectively. For each experimental condition, the enhancement in FR from each surface was calculated as

$$\text{Enhancement in FR} = (\mathrm{FR_{polymer}}/\mathrm{FR_{control}}) \times 100\% \quad (2)$$

where $\mathrm{FR_{polymer}}$ and $\mathrm{FR_{control}}$ are the percentage of fungi removed from the polymer-grafted and control surfaces, respectively. We report the average value from at least three replicates.

2.7. Oil Fouling and Removal from polyMAPS and polyMABS Brushes on Filter Paper. Silicon oil stained with Nile red (100 mg·mL^{-1}) was used as a model foulant. Paper samples were covered with 100 μL of dyed silicon oil for 2 min. To characterize the extent of release, oil-stained filter paper was rinsed with a 0.5 M NaCl solution using the same setup as for fungi experiments. Images of the samples were acquired (in similar lighting conditions) using the digital camera in dry and oil-fouled states and after rinsing the surface. For each sample, the extent of release was calculated from the converted grayscale images. Using ImageJ, the gray value index (GVI), ranging from 0 (black) to 255 (white), was quantified for each sample and averaged from at least three replicates. The oil removal (OR) percentage (removal from the surface) was calculated from the GVI of the samples in the oil-fouled ($\mathrm{GVI_F}$), rinsed ($\mathrm{GVI_R}$), and dry ($\mathrm{GVI_D}$) states as

$$\mathrm{OR} = (1 - R/F) \times 100\% \quad (3)$$

where $F = \mathrm{GVI_F} - \mathrm{GVI_D}$ and $R = \mathrm{GVI_R} - \mathrm{GVI_D}$. The enhancement in OR for each surface was calculated as

$$\text{Enhancement in OR} = (\mathrm{OR_{polymer}}/\mathrm{OR_{control}}) \times 100\% \quad (4)$$

where $\mathrm{OR_{polymer}}$ and $\mathrm{OR_{control}}$ are the OR percentage from the polymer-grafted and control surfaces, respectively. Again, we report the average value from at least three replicates.

3. RESULTS AND DISCUSSION

3.1. Synthesis of polyMAPS and polyMABS Brushes of Varying Thicknesses and Molecular Weights at Constant Grafting Density. Two series of polyMAPS (CSL = 3), and polyMABS (CSL = 4) brushes of varying molecular weights and dry thicknesses were synthesized from initiator-grafted glass coverslips or silicon substrates using SI-ATRP (Figure 1). Solution polymers (synthesized from soluble initiator present in the same reaction vessel as the glass or silicon substrates) were characterized with NMR and GPC (Figures S1) to confirm the polymer identity and quantify M_n and $Đ$, as summarized in Table S1. A wide range of molecular weights were accessed, with M_n from 19 to 1500 kg·mol^{-1}. Monomodal molecular weight distributions were achieved, with $Đ < 1.1$ for most samples (with slightly higher $Đ$ at high molecular weights). Tailing on the right side of the GPC peaks is indicative of the presence of a small amount of chain termination.

The dry thickness (ranging from 6 to 180 nm) of polyMAPS and polyMABS brushes increased with increasing M_n (Figure 2 and Table S1), as observed in prior studies[7,42,43] and attributed to stretching of the polymer chains away from the surface to avoid overlap.[44] The dry brush thickness scaled approximately linearly with M_n (Figure 2), suggesting that the grafting density was nearly constant.

We quantified the grafting density $\sigma = h\rho N_A/M_n$,[45] from the slope of the linear fit of h versus M_n, where h is the dry brush thickness, ρ = 1.34 g·cm^{-3} is the bulk density of polyMAPS and polyMABS,[7] N_A is Avogadro's number, and M_n is the molecular weight of the free polymer (with the assumption that the molecular weight of the free polymer equals that of the brush following prior studies[45−47]). σ values of polyMAPS and polyMABS brushes were determined to be 0.10 ± 0.03 and 0.16 ± 0.02 chains·nm^{-2}, respectively, which are close to values reported in previous studies that used an SI-ATRP approach.[48,42]

3.2. Distinct Wetting Behaviors of polyMAPS and polyMABS Brushes. The surface wettability was assessed via water contact angle measurements as a function of molecular weight for both polyMAPS and polyMABS brushes initially in air (Figure 3). The M_n dependences of the wetting properties were distinct for polyMAPS (CSL = 3) and polyMABS (CSL = 4). We measured both the equilibrium advancing and receding contact angles as well as a static contact angle to assess the metastable response. The advancing water contact angle θ_A of polyMAPS brushes varied between 15 and 20°, consistent with ref 49, and was nearly independent of M_n (and brush thickness) over a wide range (19−1500 kg·mol^{-1}). The

https://doi.org/10.1021/acsami.2c16417
ACS Appl. Mater. Interfaces 2023, 15, 2009−2019

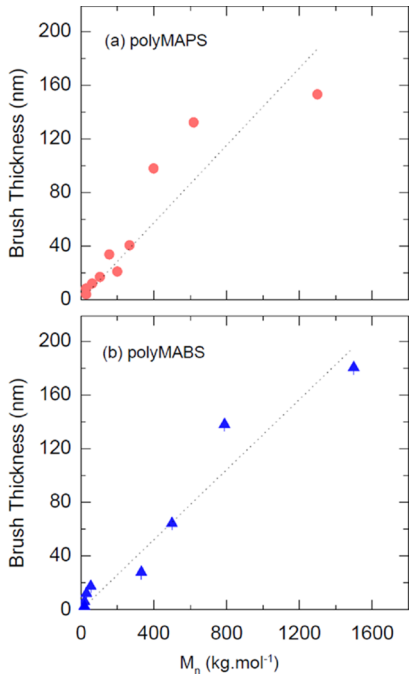

Figure 2. Dry brush thickness as a function of M_n of (a) polyMAPS and (b) polyMABS. The dashed line indicates a linear fit through the origin with R^2 = 0.89 (polyMAPS) and 0.96 (polyMABS). The grafting density σ, calculated from the slope of the linear fit, was 0.10 ± 0.03 chains nm^{-2} (polyMAPS) and 0.16 ± 0.02 chains nm^{-2} (polyMABS). Error bars represent the standard deviation of at least three measurements obtained from the same substrate and are smaller than the data point when not shown.

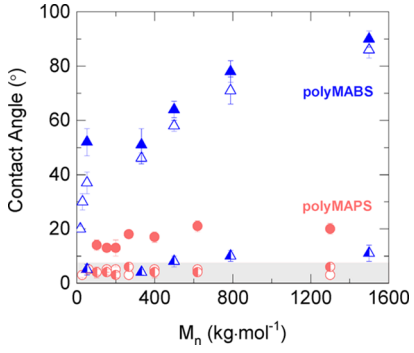

Figure 3. Advancing (solid), receding (half-filled), and static (open) water contact angle as a function of M_n for polyMAPS (red circle) and polyMABS (blue triangle). Error bars for polyMABS samples represent the standard deviation of at least three measurements obtained from the same substrate. Due to the very low water contact angles in the polyMAPS series of samples, the shaded area indicates the probable error range for these measurements. Related plots showing the dependence of contact angle on brush thickness are shown in Figure S3. Contact angles are tabulated in Table S1.

receding contact angle θ_R of polyMAPS brushes was very low and was smaller than the angular resolution limit (<10°). For this system, the static water contact angle closely tracked θ_R. By contrast, θ_A of polyMABS brushes increased from 20 to 90° as M_n increased from 19 to 1500 kg·mol^{-1}, whereas θ_R was again <10° across this range of thicknesses. This result is consistent with a previous observation that the advancing (but not receding) contact angle increased with CSL.[7] The static contact angle for polyMABS, however, closely tracked θ_A. To our knowledge, prior studies have not extensively characterized the effect of M_n (or the related brush thickness) on wetting properties in these polysulfobetaines, and the results presented in Figure 3 reveal striking differences in the behaviors of polyMAPS and polyMABS brushes. In a different zwitterionic brush system, increase in the water contact angle with increasing brush thickness was attributed to the presence of stronger intramolecular and intermolecular interactions in brushes of higher molecular weight.[50]

To explain the clear differences in the contact angles of water of polyMAPS and polyMABS, we examine prior studies on the effects of varying CSL on the properties of polyzwitterions. Ref 7 observed that the contact angle hysteresis (difference between θ_A and θ_R) was much greater for polyMABS (CSL = 4) than polyMAPS (CSL = 3) brushes and attributed this difference to slower hydration dynamics on polyMABS. In our system, we observe that θ_A for polyMABS is much greater than that for polyMAPS and, further, increases somewhat with M_n. Moreover, the metastable static contact angle tracks θ_A (which probes the hydrophobic component) for polyMABS but θ_R (which probes a hydrophilic component) for polyMAPS. Given these results, it is likely that at least part of the difference is due to slower hydration of the CSL = 4 brushes. Indeed, in captive bubble measurements [in which an air bubble of volume 10 μL was placed with a J-shaped needle on an polymer brush substrate facing downward and submerged in Milli-Q water], we were unable to trap an air bubble on either polyMAPS or polyMABS, indicating that both surfaces eventually reach similar hydration levels on very long-time scales. The origin of the slower dynamics, however, is not entirely clear. Increasing CSL is known to increase UCST due to the stronger dipole moment of the oppositely charged groups and therefore stronger interchain and/or intrachain electrostatic interactions.[6,7] We speculate that the stronger electrostatic interactions in the polyMABS (CSL = 4) brush could increase intrachain associations and reduce surface wetting relative to the polyMAPS (CSL = 3) brush. Furthermore, increasing CSL increases the hydrophobicity of the polymer and can lead to formation of cyclic structures,[2,16,51] which we hypothesize could hinder hydration of the surface. Both of these results may lead to the slower dynamics that likely underlie the greater advancing contact angle of the polyMABS brushes as compared to the polyMAPS brushes.

As the polyMABS series demonstrated a strong M_n dependence of the contact angle, we also measured the static water contact angle on selected brushes using 0.15 M and 1 M NaCl solutions (conditions relevant to bacteria fouling resistance studies) and observed no significant change in their static contact angle using the salt solution as compared to that measured in pure water (Figure S4).

3.3. Bacteria Fouling Resistance of polyMAPS and polyMABS Brushes in the Submerged State. To assess the effects of CSL and M_n on fouling resistance of polyzwitterionic brushes, we quantified the number of *S. epidermidis* bacteria cells deposited on the substrates under flow (corresponding shear stress of 24 mPa at the surface) over 30 min using confocal microscopy (Figure 4). Both polyMAPS and polyMABS brushes exhibited good resistance against fouling by bacteria, with low percentage of SC by bacteria (<5%) that was approximately independent of CSL or M_n (Figure 4). By contrast, bacteria covered an increasing percentage of the surface over time on an unmodified glass

https://doi.org/10.1021/acsami.2c16417
ACS Appl. Mater. Interfaces 2023, 15, 2009−2019

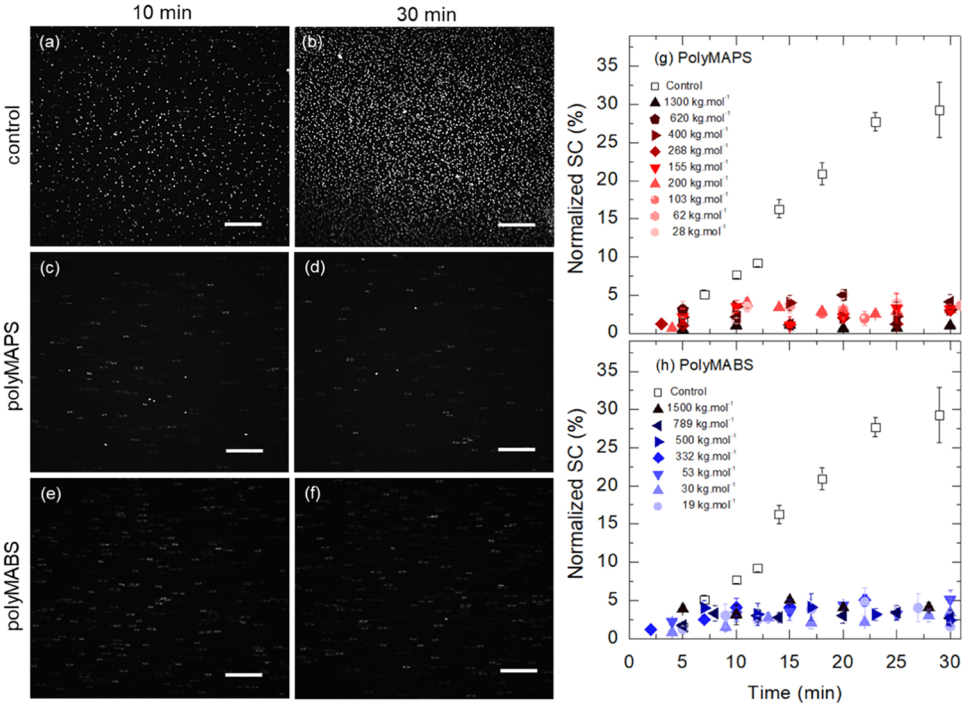

Figure 4. (a–f) Representative confocal micrographs of *S. epidermidis* bacteria deposited onto (a, b) control glass, (c, d) polyMAPS (268 kg·mol^{-1}), and (e, f) polyMABS (332 kg·mol^{-1}) brush surfaces after (a, c, e) 10 and (b, d, f) 30 min of bacteria flow over the surface in 0.15 M NaCl aqueous solution. The OD of bacteria in the salt solution was 0.9. The scale bars in the images indicate 50 μm. (g–h) Normalized SC by *S. epidermidis* bacteria on (g) polyMAPS and (h) polyMABS brushes after 30 min of incubation under flow.

substrate. This comparison demonstrates that these brushes effectively prevent fouling of surfaces by bacteria, independent of both CSL and M_n (over the ranges of each parameter studied).

Though the wetting properties of dry brushes with differing CSLs were distinct from one another (Figure 3), prior studies have demonstrated water uptake to be independent of CSL when the brushes were submerged in pure water.[7] The high resistance against fouling of both series shown in Figure 4 is likely due to their similar hydration states when submerged. Furthermore, we conducted the bacteria fouling resistance studies in a salt solution (0.15 M NaCl) to avoid osmotic shock and maintain the water balance inside cells. Prior studies on the hydration state of zwitterionic brushes in salt solutions suggested that the combination of reduced inter- and intra-chain associations and osmotic pressure effects[52] leads to even more efficient hydration of the dense brush layer (strongly depending on salt concentration and the anion or cation type).[15,43] Additionally, several studies demonstrated this efficient swelling and hydration of polyMAPS and polyMABS brushes at salt conditions relevant to the bacteria resistance experiments in our study,[15,43,47,53−55] likely contributing to the lack of bacterial fouling on these surfaces, as shown in Figure 4.

For both polyMAPS and polyMABS, there was little effect of M_n or dry brush thickness on fouling resistance across wide ranges of these parameters (Figure 4). Brushes of M_n varying from 19 to 1500 kg·mol^{-1} and of dry thickness varying from 6 to 180 nm all demonstrated low fouling. The lack of sensitivity of fouling to brush thickness can be explained by prior studies, which suggested that the hydration extent or formation of tightly bound water layer at the surface−water interface (rather than hydration through the bulk of the film) governs fouling-resistant behavior.[2,56]

3.4. Fungi Fouling Resistance of polyMAPS and polyMABS Brushes in the Submerged State. To characterize the ability of polyzwitterionic brushes to resist fouling by fungi, we deposited *A. niger* spores (whose diameter, ~10 μm, is nearly 10 times than of *S. epidermidis* bacteria) onto polyMAPS and polyMABS-grafted surfaces and quantified the number of spores on the surface before and after the chamber was inverted. (We note fungi fouling resistance studies could not be conducted in the flow cell due to fungi settling during flow.) Both polyzwitterionic brushes showed great resistance against fouling by fungi. Spores did not remain on the polyzwitterionic brush surfaces after inversion of the chamber, but instead re-suspended into solution (Figure 5). By contrast, the number of attached spores on the control sample before and after inversion were identical within statistical error. These results indicate that polyzwitterionic brushes with CSL = 3 and 4 effectively prevent fouling by larger particles such as fungi spores.

Because the inversion process removes spores from the polyzwitterionic brush surfaces, the calculated gravitational force on a settling spore can be used to estimate bounds for the attractive forces between the spores and surfaces. We estimated the gravitational force on fungi spores (67 fN) from the measured sedimentation rate for fungi spores (20.5 spores·min^{-1}; further details of these calculations are provided in the Supporting Information). The attractive force between the spore and brush surface is estimated to be less than 67 fN (since the spores are easily removed from the brush surface through sedimentation), and that between the spore and glass surface is estimated to be greater than 67 fN (in which case the spores remain on the surface when inverted).

3.5. Fouling and Fouling Release Properties of polyMAPS and polyMABS Brushes in the Dry State.

https://doi.org/10.1021/acsami.2c16417
ACS Appl. Mater. Interfaces 2023, 15, 2009−2019

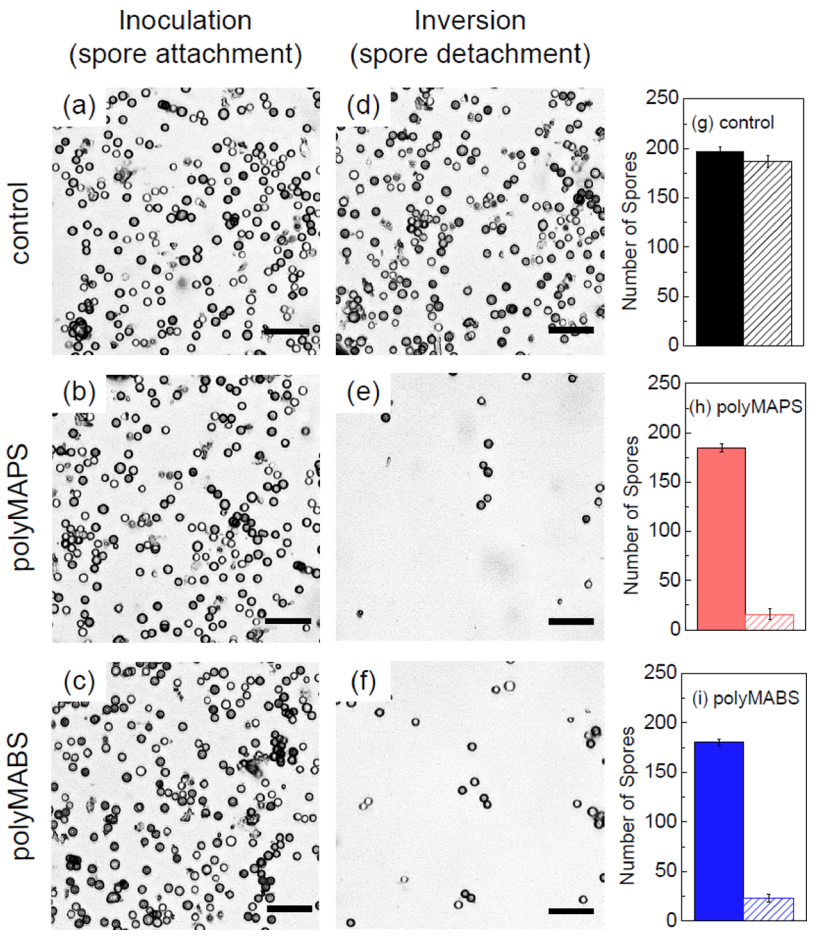

Figure 5. *Aspergillus niger* spore attachment on (a, d, g) control, (b, e, h) polyMAPS (120 kg·mol^{-1}), and (c, f, i) polyMABS (70 kg· mol^{-1}) grafted glass surfaces in 0.15 M NaCl aqueous solution. Brightfield micrographs acquired at the bottom surface (a−c) 25 min after inoculation and (d−f) after chamber inversion to remove loosely attached spores. The scale bars in the images indicate 50 μm. (g−i) Number of spores on the bottom surface after inoculation (solid) and after inversion (shaded) for (g) control, (h) polyMAPS (120 kg·mol^{-1}), and (i) polyMABS (70 kg·mol^{-1}) surfaces.

Although hydrated polyzwitterionic surfaces are known to exhibit great resistance against fouling, their performance in the dry state in air is less explored.[57] To quantify dry state properties, we grafted polyMAPS and polyMABS to filter paper because airborne fungi spores can germinate and grow on cellulose-based filter paper as a growth substrate.[41,58] We confirmed grafting of polyMAPS and polyMABS to the filter paper using ATR-FITR (Figure S5). Although we could not copolymerize in solution to measure the unbound polymer molecular weight in these syntheses, we used a similar molar ratio of monomer to the ATRP catalyst (175:1) to obtain similar chain lengths. The water contact angle on the polyMABS-grafted paper (80°) was much higher than that of the polyMAPS-grafted paper (in which the water droplet fully spread and contact angle could not be measured) (Figure S5), in agreement with the marked differences in wetting of brushes grafted to glass substrates (Figure 3). Both filter papers remained permeable to water after grafting.

A. niger colonies appeared on both polymer-grafted and bare filter paper surfaces within 4 days of incubation, as expected for microscale particles adhering in air on a solid surface[59] and consistent with prior studies quantifying adhesion of *A. niger* spores on a variety of polymer-coated substrates.[60] After 8 days of incubation, all samples were completely covered by fungi (Figure S6), confirming that fungi could metabolize the cellulose even in the presence of the grafted zwitterionic brushes. Thus, grafting of polyzwitterions did not prevent fungi attachment and growth in agar plates in air.

As polyMAPS and polyMABS brushes are effective against fouling when hydrated, we assessed whether fungi could be released from the fouled surfaces upon rinsing with water. The polyzwitterionic-grafted filter papers lightened substantially upon rinsing, whereas the blank filter paper showed little visual change (Figure 6a). We quantified the FR percentage (eq 1) from the images and found that 57 (σ = 11)% and 54 (σ = 8)% of fungi could be removed from the polyMAPS and polyMABS-grafted papers, respectively, whereas only 26 (σ = 18)% of the fungi could be removed from the bare filter paper (Figure S7). The enhancement in removal of fungi from the polyzwitterionic surfaces relative to the blank filter paper (eq 2) was therefore 219 (σ = 22)% and 207 (σ = 20)% for polyMAPS and polyMABS, respectively (Figure 6c). Thus, although polyMAPS- and polyMABS-grafted filter papers exhibited different wetting properties (Figure S5), fungi could be removed effectively from both surfaces through rinsing of the brushes. This finding is consistent with the similar fouling resistance of both surfaces when submerged (Figure 5) and also with earlier reports of efficient release of marine organisms from submerged polyMAPS brushes after rinsing.[30]

https://doi.org/10.1021/acsami.2c16417
ACS Appl. Mater. Interfaces 2023, 15, 2009−2019

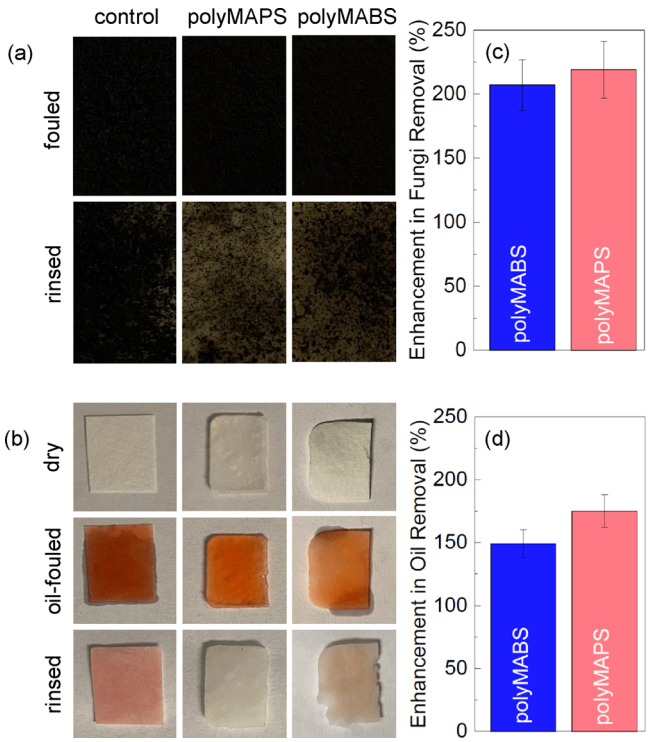

Figure 6. Representative digital images of (a) *Aspergillus niger* and (b) oil fouling of polyMAPS and polyMABS-grafted filter paper (approximate size: 1 × 2 cm) before and after rinsing, and quantification of the enhancement in (c) fungi and (d) oil removal from polyMAPS and polyMABS-grafted surfaces relative to blank filter paper. An equal amount of initiator was added during the initiator grafting step to both polyMAPS and polyMABS samples, and a similar molar ratio of monomer to the ATRP catalyst (175:1) was used in the SI-ATRP reaction to obtain similar chain lengths. Fungi and oil removal percentages are shown in Figures S7 and S8, and the rinsing setup is shown in Figure S9.

We suggest that the hydration ability of these surfaces during rinsing determines their fungi release properties. We propose that polyzwitterionic-grafted paper can hydrate more readily than the blank paper, and hydration in both polymers resulted in a similar FR. This idea is supported by prior reports indicating that the hydration ability of polyzwitterionic brushes in the wet state was independent of CSL.[7] More speculatively, steric hindrance from the polymer brushes[61,62] may have prevented fungi from accessing the paper substrate.[63,64] Fungi that were unable to enzymatically degrade the substrate (for food[65]) may have formed weaker biofilms that, in turn, were more readily released after rinsing.

Finally, we examined the resistance of the polyzwitterionic-grafted filter paper to fouling by oil. Both polyMAPS- and polyMABS-grafted surfaces facilitated removal of silicon oil (Figure 6b). The OR percentage (eq 3) of polyMAPS-grafted filter paper [109 (σ = 8)%, Figure S8] was greater than that of the blank paper control (62 (σ = 11)%), giving an enhancement in OR (eq 4) of 175 (σ = ±13)%. Notably, rinsing the polyMAPS-grafted paper almost returned the surface to its initial, pre-fouled state. Greater OR was also observed for polyMABS [80 (σ = 7)%] relative to its corresponding control [54 (σ = 9)%], resulting in an enhancement in OR of 149 (σ = 10)%. A previous report also qualitatively presented the potential of the oil release capability of a zwitterionic-grafted surface through immersion in water.[32] The greater enhancement in OR of polyMAPS relative to polyMABS is likely due to the lower contact angle of polyMAPS (Figure 3b). Oil, which interacts with the brush through van der Waals forces, is likely to displace more efficiently from the polyMAPS-grafted surface upon rinsing with water because the water binds more strongly to polyMAPS than to polyMABS.[32]

4. CONCLUSIONS

We synthesized poly(sulfobetaine) brushes of two chain spacer lengths (CSL = 3, 4) with varying molecular weights (19−1500 kg·mol^{-1}) and brush lengths (6−180 nm) and characterized their wetting and fouling resistance properties. PolyMAPS brushes (CSL = 3) were nearly completely wet by water with the contact angle close to 0, independent of molecular weight. By contrast, the surface wetting properties of polyMABS brushes (CSL = 4) depended on molecular weight, as confirmed by the increase in the contact angle with molecular weight (and brush thickness). Importantly, both polyMAPS and polyMABS showed excellent resistance against fouling by bacteria and deposition of fungi when submerged in an aqueous solution. These results suggest that both series of polymer brushes were fully hydrated when submerged and hence strongly resisted fouling, independent of molecular weight or CSL. Importantly, robust antifouling coatings may be obtained even by grafting short zwitterionic polymers to a surface. To characterize the ability of zwitterionic brushes to resist fouling in air (i.e., relevant to paints and coatings), we grafted the polymers to filter paper and examined fouling by fungi and silicon oil. Both brush-grafted surfaces became similarly fouled with *A. niger* but facilitated removal of the fungi when rinsed with a salt solution to hydrate the brushes. Surprisingly, silicon oil was removed more efficiently from the polyMAPS-grafted paper than from polyMABS-grafted paper; we speculate that this result reflects a more efficient displacement of oil by water molecules on the more hydrophilic polyMAPS brush upon rinsing. The ability to tailor the fouling and fouling-release properties of polyzwitterionic brushes via CSL and molecular weight, in both dry and submerged states, may be useful in medical, membrane, and coating technologies.

■ ASSOCIATED CONTENT

Supporting Information

The Supporting Information is available free of charge at https://pubs.acs.org/doi/10.1021/acsami.2c16417.

NMR spectra of the synthesized monomers and polymers in solution; GPC refractometer data for the unbound polymers in solution; differential scanning calorimetry and thermogravimetric analysis data for polyMABS; SI-ATRP reaction conditions and characteristics of polyMAPS and polyMABS brush samples; static, advancing, and receding water contact angles as a function of brush thickness and images of water droplets during advancing and receding measurements; polyMABS contact angle in salt solutions; schematic illustration of SI-ATRP of MAPS and MABS on filter paper and characterization with FTIR and static contact angle measurements; images of the incubated blank and polyMAPS- and polyMABS-grafted filter papers with *A. niger* spores; fungi and silicon oil removal percentage of polyMAPS and polyMABS-grafted filter paper; and

https://doi.org/10.1021/acsami.2c16417
ACS Appl. Mater. Interfaces 2023, 15, 2009−2019

calculation of the gravitational force of a sedimenting fungi spore on brushes (PDF)

S. epidermidis bacteria covering an increasing percentage of the unmodified glass surface over time (MP4)

Representative glass surface modified with a zwitterionic brush (polyMAPS, 14 nm) showing good resistance against fouling by *S. epidermidis* bacteria, with low percentage of surface coverage (<5%) (MP4)

AUTHOR INFORMATION

Corresponding Authors

Megan L. Robertson − *William A. Brookshire Department of Chemical and Biomolecular Engineering, University of Houston, Houston, Texas 77204, United States;* orcid.org/0000-0002-2903-3733; Phone: 713-743-2748; Email: mlrobertson@uh.edu

Jacinta C. Conrad − *William A. Brookshire Department of Chemical and Biomolecular Engineering, University of Houston, Houston, Texas 77204, United States;* orcid.org/0000-0001-6084-4772; Phone: 713-743-3829; Email: jcconrad@uh.edu

Authors

Fahimeh Khakzad − *William A. Brookshire Department of Chemical and Biomolecular Engineering, University of Houston, Houston, Texas 77204, United States*

Narendra K. Dewangan − *William A. Brookshire Department of Chemical and Biomolecular Engineering, University of Houston, Houston, Texas 77204, United States*

Tzu-Han Li − *William A. Brookshire Department of Chemical and Biomolecular Engineering, University of Houston, Houston, Texas 77204, United States*

Farshad Safi Samghabadi − *William A. Brookshire Department of Chemical and Biomolecular Engineering, University of Houston, Houston, Texas 77204, United States*

Ronard Herrera Monegro − *William A. Brookshire Department of Chemical and Biomolecular Engineering, University of Houston, Houston, Texas 77204, United States*

Complete contact information is available at: https://pubs.acs.org/10.1021/acsami.2c16417

Notes

The authors declare no competing financial interest.

ACKNOWLEDGMENTS

We thank Vincent Donnelly for use of the ellipsometer, Ramanan Krishnamoorti for access to the aqueous GPC, Navin Varadarajan for use of the ultra-low temperature freezers, and Simone Lupini for assistance with the fungi experiments. This research was made possible in part by grants from the American Chemical Society Petroleum Research Fund (58531-ND7) and the Welch Foundation (E-1869).

REFERENCES

(1) Xing, C.-M.; Meng, F.-N.; Quan, M.; Ding, K.; Dang, Y.; Gong, Y.-K. Quantitative fabrication, performance optimization and comparison of PEG and zwitterionic polymer antifouling coatings. *Acta Biomater.* **2017**, *59*, 129−138.

(2) Laschewsky, A.; Rosenhahn, A. Molecular Design of Zwitterionic Polymer Interfaces: Searching for the Difference. *Langmuir* **2019**, *35*, 1056−1071.

(3) Wu, A.; Gao, Y.; Zheng, L. Zwitterionic amphiphiles: their aggregation behavior and applications. *Green Chem.* **2019**, *21*, 4290−4312.

(4) Jiang, S.; Cao, Z. Ultralow-Fouling, Functionalizable, and Hydrolyzable Zwitterionic Materials and Their Derivatives for Biological Applications. *Adv. Mater.* **2010**, *22*, 920−932.

(5) Shao, Q.; Jiang, S. Molecular Understanding and Design of Zwitterionic Materials. *Adv. Mater.* **2015**, *27*, 15−26.

(6) Higaki, Y.; Kobayashi, M.; Takahara, A. Hydration State Variation of Polyzwitterion Brushes through Interplay with Ions. *Langmuir* **2020**, *36*, 9015−9024.

(7) Higaki, Y.; Inutsuka, Y.; Sakamaki, T.; Terayama, Y.; Takenaka, A.; Higaki, K.; Yamada, N. L.; Moriwaki, T.; Ikemoto, Y.; Takahara, A. Effect of Charged Group Spacer Length on Hydration State in Zwitterionic Poly(sulfobetaine) Brushes. *Langmuir* **2017**, *33*, 8404−8412.

(8) Del Grosso, C. A.; Leng, C.; Zhang, K.; Hung, H.-C.; Jiang, S.; Chen, Z.; Wilker, J. J. Surface hydration for antifouling and bioadhesion. *Chem. Sci.* **2020**, *11*, 10367−10377.

(9) Shao, Q.; He, Y.; White, A. D.; Jiang, S. Difference in Hydration between Carboxybetaine and Sulfobetaine. *J. Phys. Chem. B* **2010**, *114*, 16625−16631.

(10) Kalasin, S.; Letteri, R. A.; Emrick, T.; Santore, M. M. Adsorbed Polyzwitterion Copolymer Layers Designed for Protein Repellency and Interfacial Retention. *Langmuir* **2017**, *33*, 13708−13717.

(11) Hildebrand, V.; Laschewsky, A.; Päch, M.; Müller-Buschbaum, P.; Papadakis, C. M. Effect of the zwitterion structure on the thermoresponsive behaviour of poly(sulfobetaine methacrylates). *Polym. Chem.* **2017**, *8*, 310−322.

(12) Schlenoff, J. B. Zwitteration: Coating Surfaces with Zwitterionic Functionality to Reduce Nonspecific Adsorption. *Langmuir* **2014**, *30*, 9625−9636.

(13) Willcock, H.; Lu, A.; Hansell, C. F.; Chapman, E.; Collins, I. R.; O'Reilly, R. K. One-pot synthesis of responsive sulfobetaine nanoparticles by RAFT polymerisation: the effect of branching on the UCST cloud point. *Polym. Chem.* **2014**, *5*, 1023−1030.

(14) Hildebrand, V.; Laschewsky, A.; Wischerhoff, E. Modulating the solubility of zwitterionic poly((3-methacrylamidopropyl)-ammonioalkane sulfonate)s in water and aqueous salt solutions via the spacer group separating the cationic and the anionic moieties. *Polym. Chem.* **2016**, *7*, 731−740.

(15) Xiao, S.; Ren, B.; Huang, L.; Shen, M.; Zhang, Y.; Zhong, M.; Yang, J.; Zheng, J. Salt-responsive zwitterionic polymer brushes with anti-polyelectrolyte property. *Curr. Opin. Chem. Eng.* **2018**, *19*, 86−93.

(16) Wang, T.; Kou, R.; Liu, H.; Liu, L.; Zhang, G.; Liu, G. Anion Specificity of Polyzwitterionic Brushes with Different Carbon Spacer Lengths and Its Application for Controlling Protein Adsorption. *Langmuir* **2016**, *32*, 2698−2707.

(17) Wang, N.; Seymour, B. T.; Lewoczko, E. M.; Kent, E. W.; Chen, M.-L.; Wang, J.-H.; Zhao, B. Zwitterionic poly(sulfobetaine methacrylate)s in water: from upper critical solution temperature (UCST) to lower critical solution temperature (LCST) with increasing length of one alkyl substituent on the nitrogen atom. *Polym. Chem.* **2018**, *9*, 5257−5261.

(18) Liu, Y.; Zhang, D.; Ren, B.; Gong, X.; Xu, L.; Feng, Z.-Q.; Chang, Y.; He, Y.; Zheng, J. Molecular simulations and understanding of antifouling zwitterionic polymer brushes. *J. Mater. Chem. B* **2020**, *8*, 3814−3828.

(19) Xiao, S.; Zhang, Y.; Shen, M.; Chen, F.; Fan, P.; Zhong, M.; Ren, B.; Yang, J.; Zheng, J. Structural Dependence of Salt-Responsive Polyzwitterionic Brushes with an Anti-Polyelectrolyte Effect. *Langmuir* **2018**, *34*, 97−105.

(20) Chen, S.; Li, L.; Zhao, C.; Zheng, J. Surface hydration: Principles and applications toward low-fouling/nonfouling biomaterials. *Polymer* **2010**, *51*, 5283−5293.

(21) Azzaroni, O.; Brown, A. A.; Huck, W. T. S. UCST Wetting Transitions of Polyzwitterionic Brushes Driven by Self-Association. *Angew. Chem. Int. Ed.* **2006**, *45*, 1770−1774.

(22) Yang, Z.; Zhang, S.; Tarabara, V. V.; Bruening, M. L. Aqueous Swelling of Zwitterionic Poly(sulfobetaine methacrylate) Brushes in the Presence of Ionic Surfactants. *Macromolecules* **2018**, *51*, 1161−1171.
(23) Yang, W.; Chen, S.; Cheng, G.; Vaisocherová, H.; Xue, H.; Li, W.; Zhang, J.; Jiang, S. Film Thickness Dependence of Protein Adsorption from Blood Serum and Plasma onto Poly(sulfobetaine)-Grafted Surfaces. *Langmuir* **2008**, *24*, 9211−9214.
(24) Zhang, Z.; Vaisocherová, H.; Cheng, G.; Yang, W.; Xue, H.; Jiang, S. Nonfouling Behavior of Polycarboxybetaine-Grafted Surfaces: Structural and Environmental Effects. *Biomacromolecules* **2008**, *9*, 2686−2692.
(25) Vaisocherová, H.; Zhang, Z.; Yang, W.; Cao, Z.; Cheng, G.; Taylor, A. D.; Piliarik, M.; Homola, J.; Jiang, S. Functionalizable surface platform with reduced nonspecific protein adsorption from full blood plasma—Material selection and protein immobilization optimization. *Biosens. Bioelectron.* **2009**, *24*, 1924−1930.
(26) Zhou, X.; Koh, J. J.; He, C. Robust Oil-Fouling Resistance of Amorphous Cellulose Surface Underwater: A Wetting Study and Application. *Langmuir* **2019**, *35*, 839−847.
(27) Liu, Q.; Locklin, J. Transparent Grafted Zwitterionic Copolymer Coatings That Exhibit Both Antifogging and Self-Cleaning Properties. *ACS Omega* **2018**, *3*, 17743−17750.
(28) Knowles, B. R.; Yang, D.; Wagner, P.; Maclaughlin, S.; Higgins, M. J.; Molino, P. J. Zwitterion Functionalized Silica Nanoparticle Coatings: The Effect of Particle Size on Protein, Bacteria, and Fungal Spore Adhesion. *Langmuir* **2019**, *35*, 1335−1345.
(29) Shave, M. K.; Zhou, Y.; Kim, J.; Kim, Y. C.; Hutchison, J.; Bendejacq, D.; Goulian, M.; Choi, J.; Composto, R. J.; Lee, D. Zwitterionic surface chemistry enhances detachment of bacteria under shear. *Soft Matter* **2022**, *18*, 6618−6628.
(30) Hibbs, M. R.; Hernandez-Sanchez, B. A.; Daniels, J.; Stafslien, S. J. Polysulfone and polyacrylate-based zwitterionic coatings for the prevention and easy removal of marine biofouling. *Biofouling* **2015**, *31*, 613−624.
(31) Zhang, Z.; Finlay, J. A.; Wang, L.; Gao, Y.; Callow, J. A.; Callow, M. E.; Jiang, S. Polysulfobetaine-Grafted Surfaces as Environmentally Benign Ultralow Fouling Marine Coatings. *Langmuir* **2009**, *25*, 13516−13521.
(32) He, K.; Duan, H.; Chen, G. Y.; Liu, X.; Yang, W.; Wang, D. Cleaning of Oil Fouling with Water Enabled by Zwitterionic Polyelectrolyte Coatings: Overcoming the Imperative Challenge of Oil−Water Separation Membranes. *ACS Nano* **2015**, *9*, 9188−9198.
(33) Rahimi, A.; Stafslien, S. J.; Vanderwal, L.; Finlay, J. A.; Clare, A. S.; Webster, D. C. Amphiphilic zwitterionic-PDMS-based surface-modifying additives to tune fouling-release of siloxane-polyurethane marine coatings. *Prog. Org. Coat.* **2020**, *149*, No. 105931.
(34) Zhang, Z.; Chen, S.; Chang, Y.; Jiang, S. Surface Grafted Sulfobetaine Polymers via Atom Transfer Radical Polymerization as Superlow Fouling Coatings. *J. Phys. Chem. B* **2006**, *110*, 10799−10804.
(35) Li, T.-H.; Yadav, V.; Conrad, J. C.; Robertson, M. L. Effect of Dispersity on the Conformation of Spherical Polymer Brushes. *ACS Macro Lett.* **2021**, *10*, 518−524.
(36) Yadav, V.; Jaimes-Lizcano, Y. A.; Dewangan, N. K.; Park, N.; Li, T.-H.; Robertson, M. L.; Conrad, J. C. Tuning Bacterial Attachment and Detachment via the Thickness and Dispersity of a pH-Responsive Polymer Brush. *ACS Appl. Mater. Interfaces* **2017**, *9*, 44900−44910.
(37) Liu, P.; Chen, Q.; Li, L.; Lin, S.; Shen, J. Anti-biofouling ability and cytocompatibility of the zwitterionic brushes-modified cellulose membrane. *J. Mater. Chem. B* **2014**, *2*, 7222−7231.
(38) Liu, P.-S.; Chen, Q.; Liu, X.; Yuan, B.; Wu, S.-S.; Shen, J.; Lin, S.-C. Grafting of Zwitterion from Cellulose Membranes via ATRP for Improving Blood Compatibility. *Biomacromolecules* **2009**, *10*, 2809−2816.
(39) Huhtamäki, T.; Tian, X.; Korhonen, J. T.; Ras, R. H. A. Surface-wetting characterization using contact-angle measurements. *Nat. Protoc.* **2018**, *13*, 1521−1538.
(40) Sharma, S.; Conrad, J. C. Attachment from Flow of Escherichia coli Bacteria onto Silanized Glass Substrates. *Langmuir* **2014**, *30*, 11147−11155.
(41) Xu, J.; Bai, Y.; Wan, M.; Liu, Y.; Tao, L.; Wang, X. Antifungal Paper Based on a Polyborneolacrylate Coating. *Polymers* **2018**, *10*, 448.
(42) Terayama, Y.; Kikuchi, M.; Kobayashi, M.; Takahara, A. Well-Defined Poly(sulfobetaine) Brushes Prepared by Surface-Initiated ATRP Using a Fluoroalcohol and Ionic Liquids as the Solvents. *Macromolecules* **2011**, *44*, 104−111.
(43) Sakamaki, T.; Inutsuka, Y.; Igata, K.; Higaki, K.; Yamada, N. L.; Higaki, Y.; Takahara, A. Ion-Specific Hydration States of Zwitterionic Poly(sulfobetaine methacrylate) Brushes in Aqueous Solutions. *Langmuir* **2019**, *35*, 1583−1589.
(44) Yamaguchi, H.; Honda, K.; Kobayashi, M.; Morita, M.; Masunaga, H.; Sakata, O.; Sasaki, S.; Takahara, A. Molecular Aggregation State of Surface-grafted Poly{2-(perfluorooctyl)ethyl acrylate} Thin Film Analyzed by Grazing Incidence X-ray Diffraction. *Polym. J.* **2008**, *40*, 854−860.
(45) Wu, T.; Gong, P.; Szleifer, I.; Vlček, P.; Šubr, V.; Genzer, J. Behavior of Surface-Anchored Poly(acrylic acid) Brushes with Grafting Density Gradients on Solid Substrates: 1. Experiment. *Macromolecules* **2007**, *40*, 8756−8764.
(46) Treat, N. D.; Ayres, N.; Boyes, S. G.; Brittain, W. J. A Facile Route to Poly(acrylic acid) Brushes Using Atom Transfer Radical Polymerization. *Macromolecules* **2006**, *39*, 26−29.
(47) Lego, B.; Skene, W. G.; Giasson, S. Swelling Study of Responsive Polyelectrolyte Brushes Grafted from Mica Substrates: Effect of pH, Salt, and Grafting Density. *Macromolecules* **2010**, *43*, 4384−4393.
(48) Kobayashi, M.; Terayama, Y.; Kikuchi, M.; Takahara, A. Chain dimensions and surface characterization of superhydrophilic polymer brushes with zwitterion side groups. *Soft Matter* **2013**, *9*, 5138−5148.
(49) Kobayashi, M.; Terayama, Y.; Yamaguchi, H.; Terada, M.; Murakami, D.; Ishihara, K.; Takahara, A. Wettability and Antifouling Behavior on the Surfaces of Superhydrophilic Polymer Brushes. *Langmuir* **2012**, *28*, 7212−7222.
(50) Cheng, N.; Brown, A. A.; Azzaroni, O.; Huck, W. T. S. Thickness-Dependent Properties of Polyzwitterionic Brushes. *Macromolecules* **2008**, *41*, 6317−6321.
(51) Izumrudov, V. A.; Domashenko, N. I.; Zhiryakova, M. V.; Davydova, O. V. Interpolyelectrolyte Reactions in Solutions of Polycarboxybetaines, 2: Influence of Alkyl Spacer in the Betaine Moieties on Complexing with Polyanions. *J. Phys. Chem. B* **2005**, *109*, 17391−17399.
(52) Murakami, D.; Kobayashi, M.; Higaki, Y.; Jinnai, H.; Takahara, A. Swollen structure and electrostatic interactions of polyelectrolyte brush in aqueous solution. *Polymer* **2016**, *98*, 464−469.
(53) Víšová, I.; Vrabcová, M.; Forinová, M.; Zhigunová, Y.; Mironov, V.; Houska, M.; Bittrich, E.; Eichhorn, K.-J.; Hashim, H.; Schovánek, P.; Dejneka, A.; Vaisocherová-Lísalová, H. Surface Preconditioning Influences the Antifouling Capabilities of Zwitterionic and Nonionic Polymer Brushes. *Langmuir* **2020**, *36*, 8485−8493.
(54) Delgado, J. D.; Schlenoff, J. B. Static and Dynamic Solution Behavior of a Polyzwitterion Using a Hofmeister Salt Series. *Macromolecules* **2017**, *50*, 4454−4464.
(55) Kikuchi, M.; Terayama, Y.; Ishikawa, T.; Hoshino, T.; Kobayashi, M.; Ohta, N.; Jinnai, H.; Takahara, A. Salt Dependence of the Chain Stiffness and Excluded-Volume Strength for the Polymethacrylate-Type Sulfopropylbetaine in Aqueous NaCl Solutions. *Macromolecules* **2015**, *48*, 7194−7204.
(56) Chapman, R. G.; Ostuni, E.; Takayama, S.; Holmlin, R. E.; Yan, L.; Whitesides, G. M. Surveying for Surfaces that Resist the Adsorption of Proteins. *J. Am. Chem. Soc.* **2000**, *122*, 8303−8304.
(57) Wang, C.; Ma, C.; Mu, C.; Lin, W. Tailor-made zwitterionic polyurethane coatings: microstructure, mechanical property and their antimicrobial performance. *RSC Adv.* **2017**, *7*, 27522−27529.

https://doi.org/10.1021/acsami.2c16417
ACS Appl. Mater. Interfaces 2023, 15, 2009−2019

(58) El Bergadi, F.; Laachari, F.; Elabed, K; Mohammad, I. H.; Ibnsouda, S. K. Cellulolytic potential and filter paper activity of fungi isolated from ancients manuscripts from the Medina of Fez. *Ann. Microbiol.* **2014**, *64*, 815−822.
(59) Israelachvili, J. N.*Intermolecular and Surface Forces*; Elsevier, Academic Press: 2011.
(60) Whitehead, K. A.; Deisenroth, T.; Preuss, A.; Liauw, C. M.; Verran, J. The effect of surface properties on the strength of attachment of fungal spores using AFM perpendicular force measurements. *Colloids Surf., B* **2011**, *82*, 483−489.
(61) Roosjen, A.; van der Mei, H. C.; Busscher, H. J.; Norde, W. Microbial Adhesion to Poly(ethylene oxide) Brushes: Influence of Polymer Chain Length and Temperature. *Langmuir* **2004**, *20*, 10949−10955.
(62) Inoue, Y.; Nakanishi, T.; Ishihara, K. Elastic Repulsion from Polymer Brush Layers Exhibiting High Protein Repellency. *Langmuir* **2013**, *29*, 10752−10758.
(63) Leckband, D.; Sheth, S.; Halperin, A. Grafted poly(ethylene oxide) brushes as nonfouling surface coatings. *J. Biomater. Sci., Polym. Ed.* **1999**, *10*, 1125−1147.
(64) Nejadnik, M. R.; van der Mei, H. C.; Norde, W.; Busscher, H. J. Bacterial adhesion and growth on a polymer brush-coating. *Biomaterials* **2008**, *29*, 4117−4121.
(65) Daly, P.; Peng, M.; Mitchell, H. D.; Kim, Y.-M.; Ansong, C.; Brewer, H.; de Gijsel, P.; Lipton, M. S.; Markillie, L. M.; Nicora, C. D.; Orr, G.; Wiebenga, A.; Hildén, K. S.; Kabel, M. A.; Baker, S. E.; Mäkelä, M. R.; de Vries, R. P. Colonies of the fungus Aspergillus niger are highly differentiated to adapt to local carbon source variation. *Environ. Microbiol.* **2020**, *22*, 1154−1166.

https://doi.org/10.1021/acsami.2c16417
ACS Appl. Mater. Interfaces 2023, 15, 2009−2019